ALMA Memo XXX
The accuracy of Single Load Calibration

S.Guilloteau (IRAM / ESO)

October 22, 2002

Abstract

This memos contains a detailed evaluation of the expected performance of the single load calibration device. These performances are considered with respect to two different goals: absolute and relative calibration.

The single load calibation scheme offers an accurate compensation for the atmospheric opacity variations. However, it is sensitive to the thermal structure of the atmosphere.

1 Basic Equations

1.1 Standard Chopper / Vane Calibration

The calibration can be derived from the output powers measured by the receiver on the sky $P_{\rm sky}$ and when looking at a load $P_{\rm load}$, compared to the correlated signal measured by the correlator, $C_{\rm source}$:

$$\begin{aligned} P_{\rm sky} &= K(T)(T_{\rm rec} + J_{\rm sky}) \\ P_{\rm load} &= K(T)(T_{\rm rec} + fJ_{\rm load} + (1-f)J_{\rm sky}) \\ C_{\rm source} &= K(T)g_s\eta e^{-\tau}T_A \end{aligned} \tag{1}$$

The coefficient $K(T)$ incorporates possible non linearity of the detector (receiver + amplifiers + backend). f is the fraction of the beam filled by the load, and η the forward efficiency. g_s and g_i are the normalized signal and image gain of the receivers $g_s + g_i = 1$. Note that, in terms of image to signal sideband gain ratio, g,

$$g_s = 1/(1+g) \quad \text{and} \quad g_i = g/(1+g) \tag{2}$$

The sky emissivity $J_{\rm sky}$ is given by

$$\begin{aligned} J_{\rm sky} &= g_s(\eta J^s_{\rm m}(1-e^{-\tau_s}) + \eta J^s_{\rm bg}e^{-\tau_s} + (1-\eta)J^s_{\rm spill}) \\ &\quad + g_i(\eta J^i_{\rm m}(1-e^{-\tau_i}) + \eta J^i_{\rm bg}e^{-\tau_i} + (1-\eta)J^i_{\rm spill}) \end{aligned} \tag{3}$$

where τ_j is the sky opacity (at the current elevation) and

$$J^j_{\rm x} = \frac{h\nu_j}{k}\frac{1}{e^{h\nu_j/kT_{\rm x}}-1} \tag{4}$$

is the Rayleigh-Jeans equivalent temperature of a black body at $T_{\rm x}$ at frequency ν_j. j takes values s or i for signal or image bands respectively. $J_{\rm m}$ is the effective sky temperature, $J_{\rm bg}$

the cosmic background, and $J_{\rm spill}$ the spillover. Similarly, the effective load temperature $J_{\rm load}$ is

$$J_{\rm load} = g_s J^s_{\rm load} + g_i J^i_{\rm load} \tag{5}$$

Avoiding saturation problems has been discussed in details in [Guilloteau & Moreno, memo 371] [Guilloteau, memo 423], so that saturation will be ignored here. There are two basic modes of calibration: the single-load technique, which uses an a priori knowledge of the sky effective temperature, and the dual-load technique, which derives the receiver gain from two loads at differing temperatures.

2 Single Load

In the single-load technique, the source antenna temperature is given by

$$T_A = T_{\rm cal} \frac{C_{\rm source}}{P_{\rm load} - P_{\rm sky}} \tag{6}$$

where $T_{\rm cal}$ is the calibration temperature [Ulich & Haas, 1976]. From Eq.2, one can easily express $T_{\rm cal}$ as

$$\begin{aligned} T_{\rm cal} &= \frac{e^{\tau_s}}{\eta g_s} f (J_{\rm load} - J_{\rm sky}) & (7)\\ &= \frac{e^{\tau_s}}{\eta g_s} f (g_s J^s_{\rm load} + g_i J^i_{\rm load} \\ &- g_s (\eta J^s_{\rm m} (1 - e^{-\tau_s}) + \eta J^s_{\rm bg} e^{-\tau_s} + (1-\eta) J^s_{\rm spill}) \\ &- g_i (\eta J^i_{\rm m} (1 - e^{-\tau_i}) + \eta J^i_{\rm bg} e^{-\tau_i} + (1-\eta) J^i_{\rm spill}) \ ) & (8) \end{aligned}$$

The coupling factor to the load, f, appears as a simple scaling factor in $T_{\rm cal}$, and will just be set to 1 in the following equations for simplicity. Eq.8, after some (tedious) re-arrangement is strictly equivalent to the following one

$$\begin{aligned} T_{\rm cal} &= J^s_{\rm spill} - J^s_{\rm bg} + g (J^i_{\rm spill} - J^i_{\rm bg}) \\ &+ (e^{\tau_s} - 1)(J^s_{\rm spill} - J^s_{\rm m} + g (J^i_{\rm spill} - J^i_{\rm m})) \\ &+ g (e^{\tau_s - \tau_i} - 1)(J^i_{\rm m} - J^i_{\rm bg}) \\ &+ \frac{e^{\tau_s}}{\eta} (J^s_{\rm load} - J^s_{\rm spill} + g (J^i_{\rm load} - J^i_{\rm spill})) \end{aligned} \tag{9}$$

where g is the image to signal band ratio ($g_s = 1/(1+g)$, and $g_i = g/(1+g)$. Eq.9 allows to put in better perspective the effect of the various parameters.

The expression of $T_{\rm cal}$, although complex, has some useful limiting cases, which are convenient to remember important parameters. Eq.9 can further be (simply) re-arranged to explicitly separate two terms, one which depends on the opacity difference between the signal and image bands and one which does not.

$$\begin{aligned} T_{\rm cal} &= J^s_{\rm spill} - J^s_{\rm bg} + g (J^i_{\rm spill} - J^i_{\rm bg}) \\ &+ (e^{\tau_s} - 1)(J^s_{\rm spill} - J^s_{\rm m} + g (J^i_{\rm spill} - J^i_{\rm m})) \\ &+ \frac{e^{\tau_s}}{\eta} (J^s_{\rm load} - J^s_{\rm spill} + g (J^i_{\rm load} - J^i_{\rm spill})) \\ &+ g (e^{\tau_s - \tau_i} - 1)(J^i_{\rm m} - J^i_{\rm bg}) \end{aligned} \tag{10}$$

2.1 The simple approximations

Furthermore, with $\tau_s = \tau_i = \tau$, ignoring the weak differences between image and signal band for the various equivalent temperatures gives

$$T_{\rm cal} = (1+g)\left(J_{\rm spill} - J_{\rm bg} + (e^{\tau}-1)(J_{\rm spill} - J_{\rm m}) + \frac{e^{\tau}}{\eta}(J_{\rm load} - J_{\rm spill})\right) \tag{11}$$

from which one can derive simple approximations in two useful cases: the homogeneous temperature case $J_{\rm load} \simeq J_{\rm m} \simeq J_{\rm spill}$ for which

$$T_{\rm cal} \simeq (1+g)J_{\rm m} \tag{12}$$

and the low opacity case $\tau \ll 1$, for which

$$T_{\rm cal} \simeq \frac{1+g}{\eta}(J_{\rm load} - (1-\eta)J_{\rm spill}) \tag{13}$$

This simplified formulas show that the accuracy of the calibration will be controlled by different parameters depending on whether the atmosphere is very transparent, or significantly optically thick.

2.2 Partial Derivatives

Eq.10 actually shows the dependence on $T_{\rm cal}$ on all the independent parameters, which are $\eta, J_{\rm spill}, J_{\rm m}, J_{\rm load}, g$ and to first order $\tau_s, \tau_s - \tau_i$. τ_s and τ_i are not adequate independent parameters, because the opacity of the atmosphere is due to wide absorption lines which imply a strong correlation between opacities at different frequencies.

Derivatives relative to η

$$\frac{\partial T_{\rm cal}}{\partial \eta} = -\frac{e^{\tau_s}}{\eta^2}(J^s_{\rm load} - J^s_{\rm spill} + g(J^i_{\rm load} - J^i_{\rm spill})) \tag{14}$$

$$\simeq -\frac{e^{\tau_s}}{\eta^2}(1+g)(J_{\rm spill} - J_{\rm load}) \tag{15}$$

Derivatives relative to τ_s

$$\frac{\partial T_{\rm cal}}{\partial \tau_s} = e^{\tau_s}(J^s_{\rm spill} - J^s_{\rm m} + g(J^i_{\rm spill} - J^i_{\rm m})) + \frac{e^{\tau_s}}{\eta}(J^s_{\rm load} - J^s_{\rm spill} + g(J^i_{\rm load} - J^i_{\rm spill}))$$
$$- (e^{\tau_s}-1)\frac{\partial J^s_{\rm m}}{\partial \tau_s} - g(e^{\tau_i}-1)\frac{\partial J^i_{\rm m}}{\partial \tau_s} \tag{16}$$

$$\simeq \frac{e^{\tau_s}(1+g)}{\eta}\left(\eta(J_{\rm spill} - J_{\rm m}) + (J_{\rm load} - J_{\rm spill})\right) \tag{17}$$

Derivatives relative to $T_{\rm load}$

$$\frac{\partial T_{\rm cal}}{\partial T_{\rm load}} = \frac{e^{\tau_s}}{\eta}\left(\frac{\partial J^s_{\rm load}}{\partial T_{\rm load}} + g\frac{\partial J^i_{\rm load}}{\partial T_{\rm load}}\right) \tag{18}$$

$$\simeq \frac{e^{\tau_s}}{\eta}(1+g) \tag{19}$$

Derivatives relative to $J_{\rm m}$, assuming $J^s_{\rm m} \approx J^i_{\rm m} = J_{\rm m}$

$$\frac{\partial T_{\rm cal}}{\partial J_{\rm m}} = -(e^{\tau_s}-1)(1+g) + g(e^{\tau_s - \tau_i} - 1) \tag{20}$$

$$
\begin{aligned}
T_{\rm cal} &= J^s_{\rm spill} - J^s_{\rm bg} + g(J^i_{\rm spill} - J^i_{\rm bg}) \\
&+ (e^{\tau_s} - 1)(J^s_{\rm spill} - J^s_{\rm m} + g(J^i_{\rm spill} - J^i_{\rm m})) \\
&+ \frac{e^{\tau_s}}{\eta}(J^s_{\rm load} - J^s_{\rm spill} + g(J^i_{\rm load} - J^i_{\rm spill})) \\
&+ g(e^{\tau_s - \tau_i} - 1)(J^i_{\rm m} - J^i_{\rm bg}) \qquad (21)
\end{aligned}
$$

Fig.1 gives the dependence of the various effective temperatures $J_{\rm m}$, $J_{\rm spill}$ and $J_{\rm load}$ with the frequency. Since the difference in frequency between the sidebands of ALMA receivers vary between 8 and 24 GHz, these curves can be used to verify how valid is the approximation $J^s_{\rm m} = J^i_{\rm m}$. Differences are in general very small (typically less than 2 K, i.e. 1 %), smaller than 5 K except when one sideband falls in a spectral line, in which case the difference can reach about 10 K.

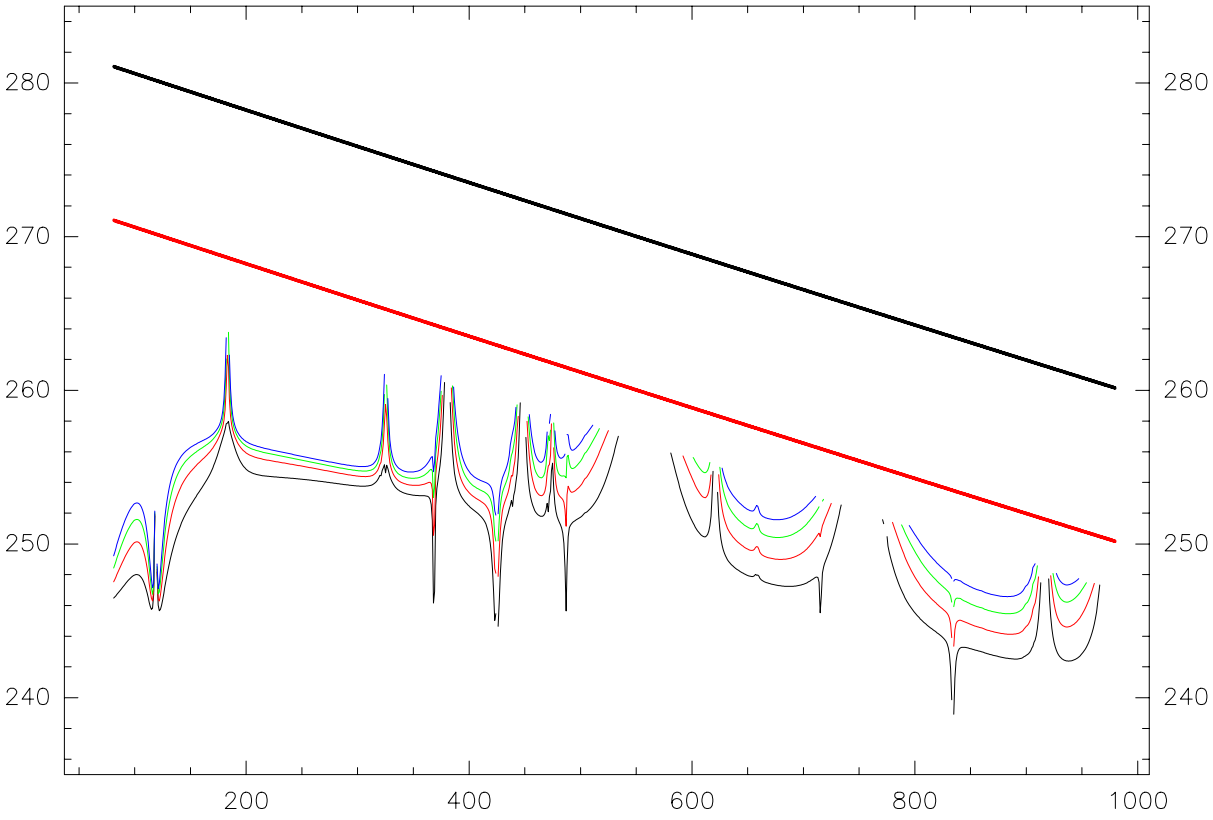

Figure 1: Dependency of the effective temperatures as function of frequency. $J_{\rm load}$ is the thick black line, $J_{\rm spill}$ the thick red line, and the 4 curves with different colors are $J_{\rm m}$ for 4 different water vapor content (0.5, 1, 1.5, 2 mm, from bottom to top). Outside temperature is 273 K, load temperature 283 K.

Another important aspect is the variation of $J_{\rm m}$ with atmospheric parameters. Fig.2 gives the dependence of $J_{\rm m}$ with the outside ground-level air temperature for 4 different frequencies. The cloud of points for each frequency corresponds to different water vapor content. Fig.3 gives the corresponding dependence in terms of airmasses.

Fig.1-3 uses the "old" ATM model from Cernicharo (1985) and ignore a number of minor constituents in the atmosphere. This will change the detailed behavior of $J_{\rm m}(\nu)$, by adding a number of small narrow lines from e.g. ozone, but not the magnitude of the effects: variations

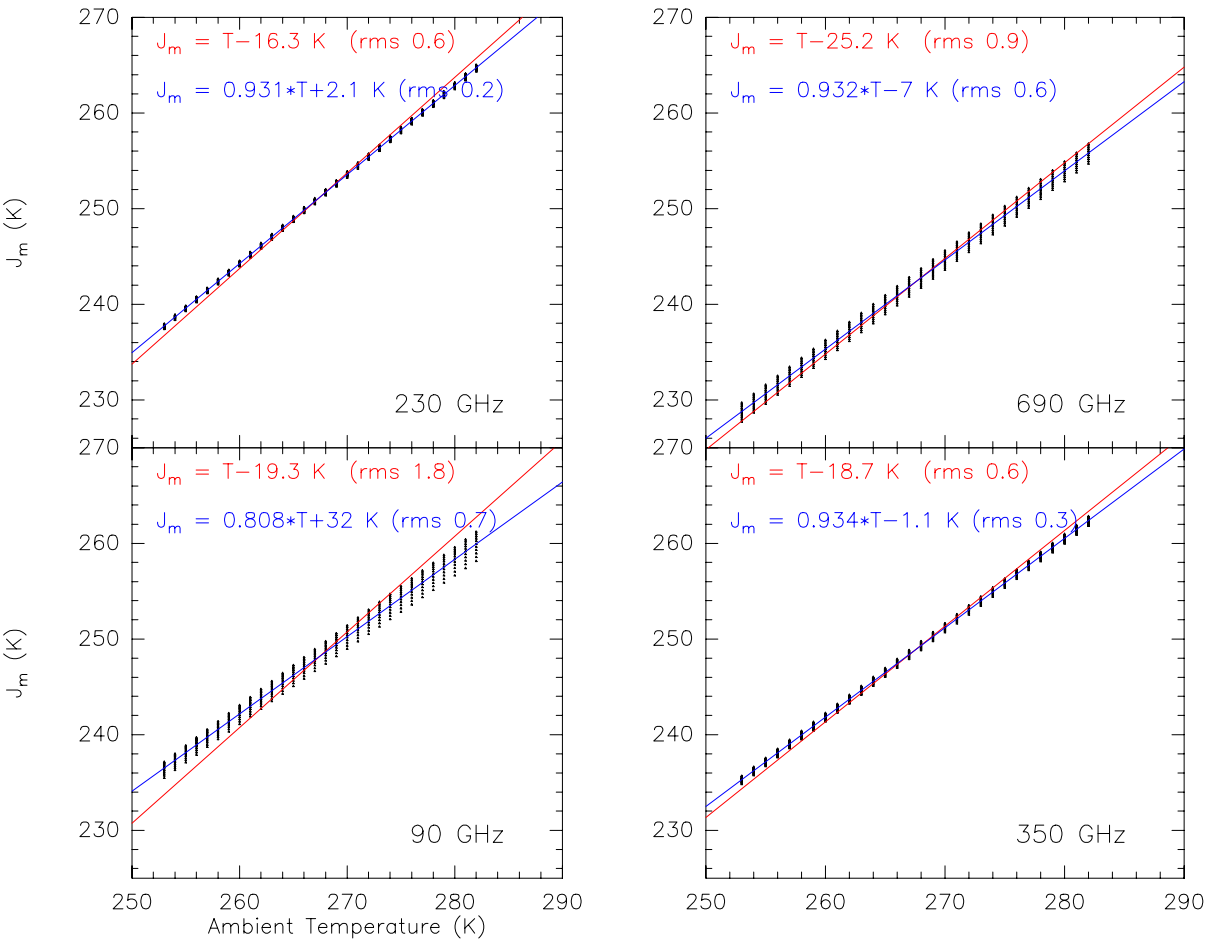

Figure 2: Dependency of the atmospheric temperature as function of ground temperature

of $J_{\rm m}$ will remain small.

2.3 $T_{\rm cal}$ values

As shown by Eq.11, the best way to minimize errors on $T_{\rm cal}$ due to varying atmospheric conditions is to try to reach the homogeneous conditions. This is never strictly possible if ambient loads are used, because the atmosphere is always colder than the ground temperature, and a fortiori than the receiver cabin. A good practice to minimize the errors is nevertheless to use a relatively cold receiver cabin, e.g. 10°C or so. All figures presented here uses this value unless specified.

Values of $T_{\rm cal}$ (or more precisely of $T_{\rm cal}/(1+g)$ which is the parameter relevant for continuum calibration) as a function of several parameters (frequency ν, water vapor content, load temperature) are given in Fig.4-8. This assumes "standard" parameters for the ALMA receiver, namely $g \simeq 0.1$ up to Band 7, and $g \simeq 1$ above. The calibration accuracy goals of 1 and 3 % for mm and submm wavelengths are indicated in Fig.4. The 1 % goal is achievable at mm frequencies under these conditions. Somewhat better atmospheric transparency (< 1.5 mm) is required near 350 GHz. Fig.5 gives a similar plot for submm observing conditions (water vapor ranging from 0.35 to 0.65 mm), showing that the 3 % goal should be achievable at least in the most transparent parts of the submm windows.

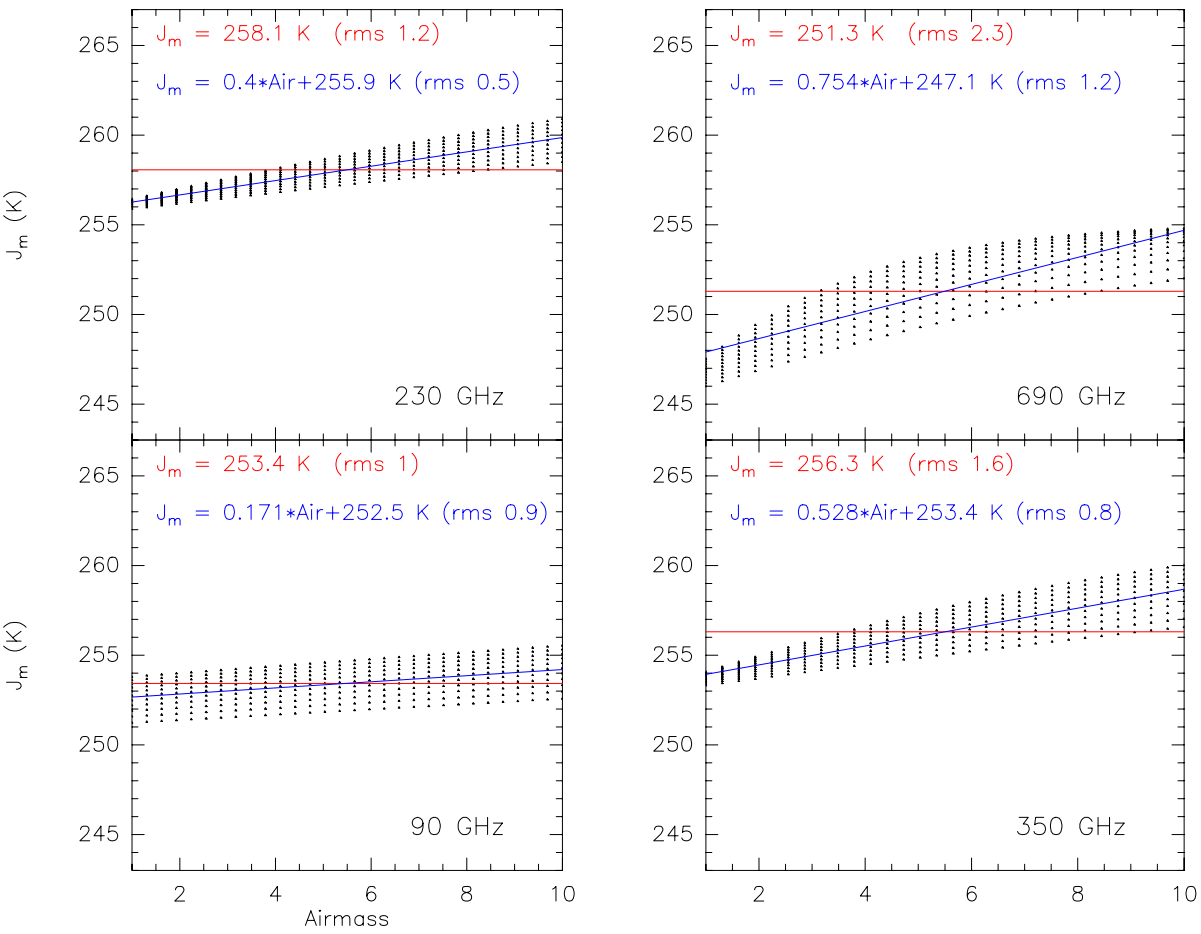

Figure 3: Dependency of the atmospheric temperature as function of number of air masses

Another aspect which is important for the amplitude calibration is the dependence of $T_{\rm cal}$ on the elevation, since the flux calibrators (primary or secondary) are not exactly at the source elevation. Figure **??** shows this dependence for airmasses of 1, 1.2, 1.44, 2, 3 and 5, corresponding to elevations of $90°, 56°, 44°, 30°, 19°$ and $11°$ respectively. The water vapor content is assumed to correspond to the appropriate observing conditions, i.e. < 2.3 mm for Band 3 and 6, < 1.5 for Band 7, and < 0.5 mm for Band 9 and 10.

In general, $T_{\rm cal}$ is weakly dependent on the water vapor content and number of airmasses, i.e. on the atmospheric opacity. Weak lines from e.g. ozone could have a very small effect on $J_{\rm m}$, specially if they originate from the upper layers of the atmosphere. However, such narrow lines will have an important effect on $T_{\rm cal}$ through the opacity difference term (see Eq.11). A line of opacity $\Delta\tau$ will change $T_{\rm cal}$ by

$$\Delta T_{\rm cal} = g\Delta\tau J_{\rm m} \quad (22)$$

$$\frac{\Delta T_{\rm cal}}{T_{\rm cal}} \approx \frac{g}{1+g}\Delta\tau \quad (23)$$

This can be a big effect, specially in the sub-mm domain where sideband separating receivers are difficult to build, so that $g \simeq 1$. Matching the required precision will thus imply accurate predictions of all (narrow) line opacities. Since these atmospheric lines are of order a few 100 MHz wide, it is important for ALMA to implement a calibration scheme which applies a $T_{\rm cal}$

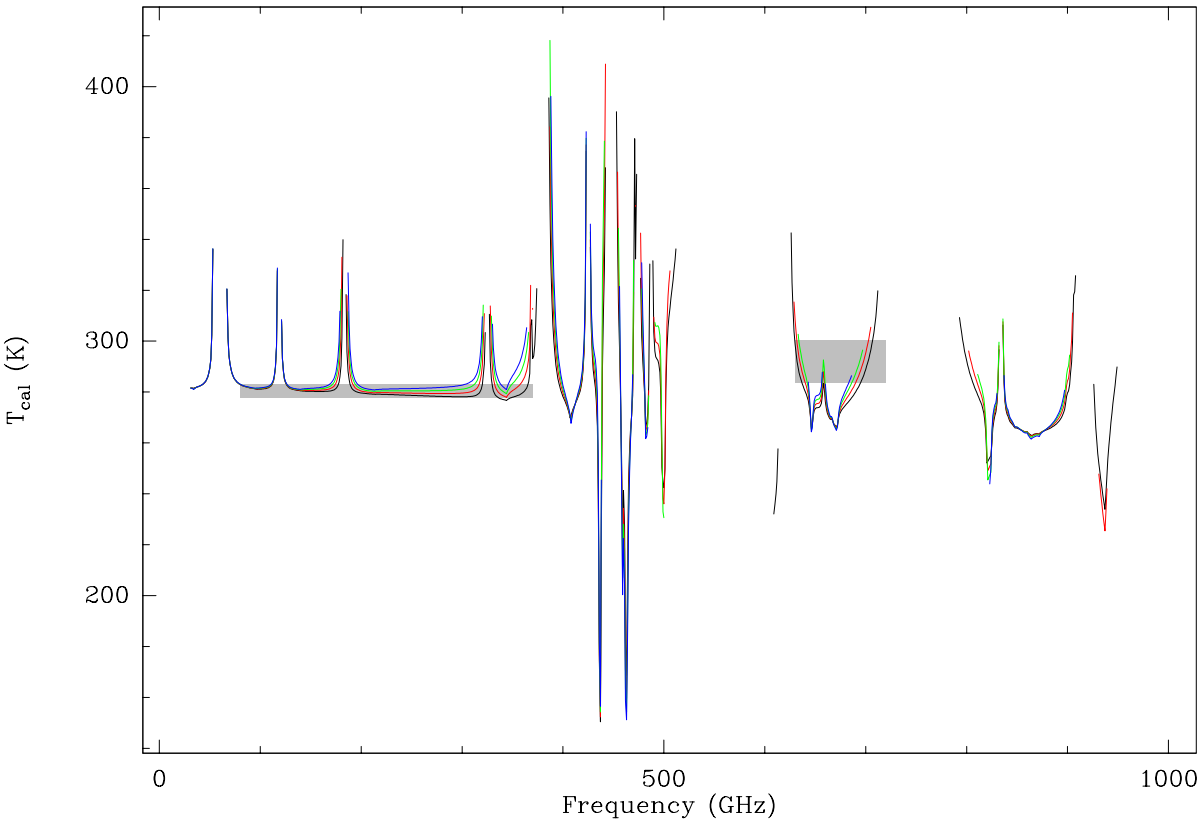

Figure 4: Dependency of the $T_{\rm cal}$ factor as function of frequency for a load temperature of 283 K. Curves are given for 4 water vapor content: 0.5 mm (black), 1 mm (red), 1.5 mm (green) and 2 mm (blue). The grey areas indicate the $\pm 1\%$ error level at mm wavelengths, and the $\pm 3\%$ error level for band 9.

factor at this spectral resolution. This implies using the correlator in all circumstances, relying on the continuum detectors only in a secondary way.

3 Dual-Load Calibration

In the dual-load calibration system, a cold and an ambient temperature loads are used in general.

$$P_{\rm hot} = K(T)(T_{\rm rec} + J_{\rm cold}) \quad (24)$$

$$P_{\rm amb} = K(T)(T_{\rm rec} + J_{\rm amb}) \quad (25)$$

$$C_{\rm source} = K(T) g_s \eta e^{-\tau} T_A \quad (26)$$

Eliminating the electronic gain $K(T)$ (ignoring saturation at this stage) gives

$$T_A = \frac{e^{\tau}}{g_s \eta}(J_{\rm amb} - J_{\rm cold}) \frac{C_{\rm source}}{P_{\rm amb} - P_{\rm cold}} = T_{\rm cal} \frac{C_{\rm source}}{P_{\rm amb} - P_{\rm cold}} \quad (27)$$

where the calibration temperature is now

$$T_{\rm cal} = \frac{(1+g)e^{\tau}}{\eta}(J_{\rm amb} - J_{\rm cold}) \quad (28)$$

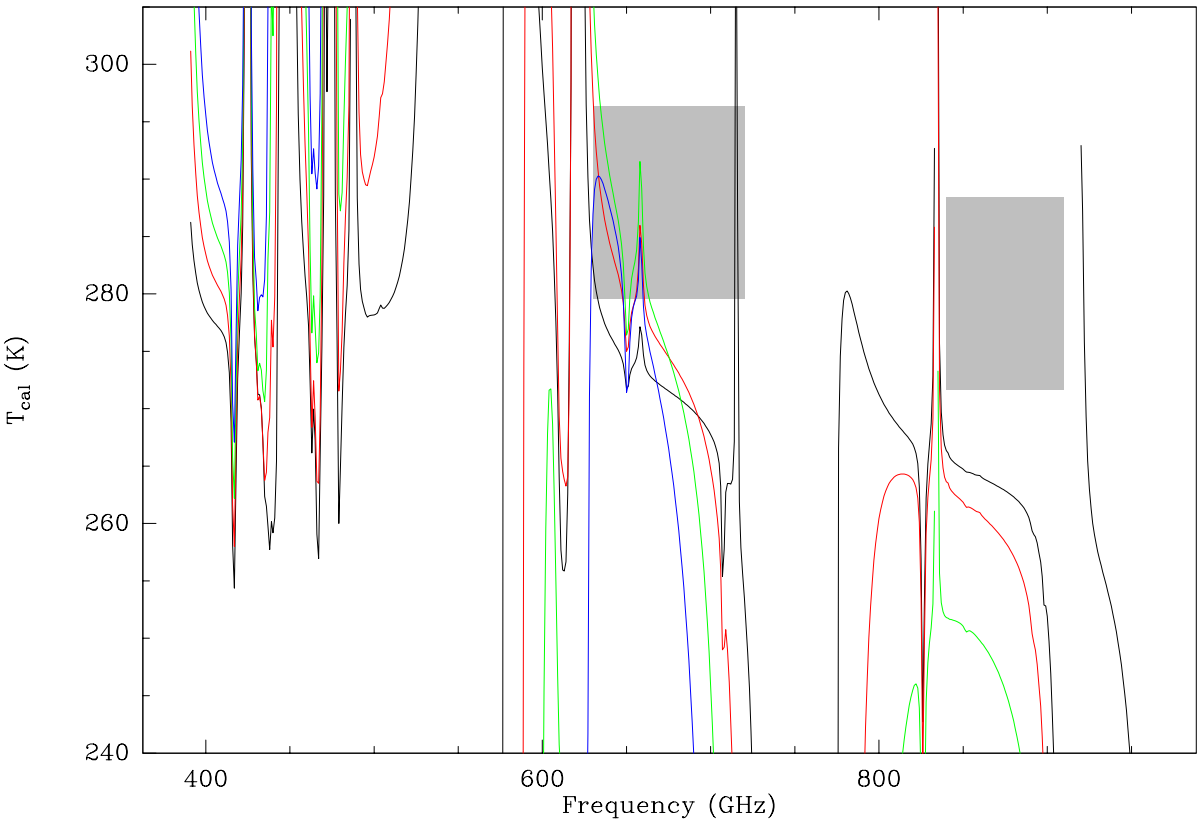

Figure 5: Dependency of the $T_{\rm cal}$ factor as function of frequency for a load temperature of 283 K. Curves are given for 4 water vapor content: 0.35 mm (black), 0.45 mm (red), 0.55 mm (green) and 0.65 mm (blue). The grey areas indicate the ±3% error level for Band 9 and 10.

Accurate calibration requires accurate knowledge of τ, η and of the effective load temperatures. The latter is a difficult problem, because of the nature of a cold load. Cold loads require some insulated box, and an optical device to couple all the beam to the load as assumed in Eq.24. Both are non trivial problems. The insulation requires an opaque material in the infrared, but transparent in the sub-mm domain. For example, if the cold load is made through a window looking into the dewar, at a temperature of about 70–80 K, an error on the cold load temperature by 1 K gives an error on $T_{\rm cal}$ shown in Fig.**??**.

4 Conclusions

References

[Mangum memo 318]
Mangum, J. 2000
Amplitude Calibration at Millimeter and Sub-millimeter Wavelengths *ALMA memo 318*

[Plambeck memo 321]
Plambeck, R., 2000
Receiver Amplitude Calibration for ALMA *ALMA memo 321*

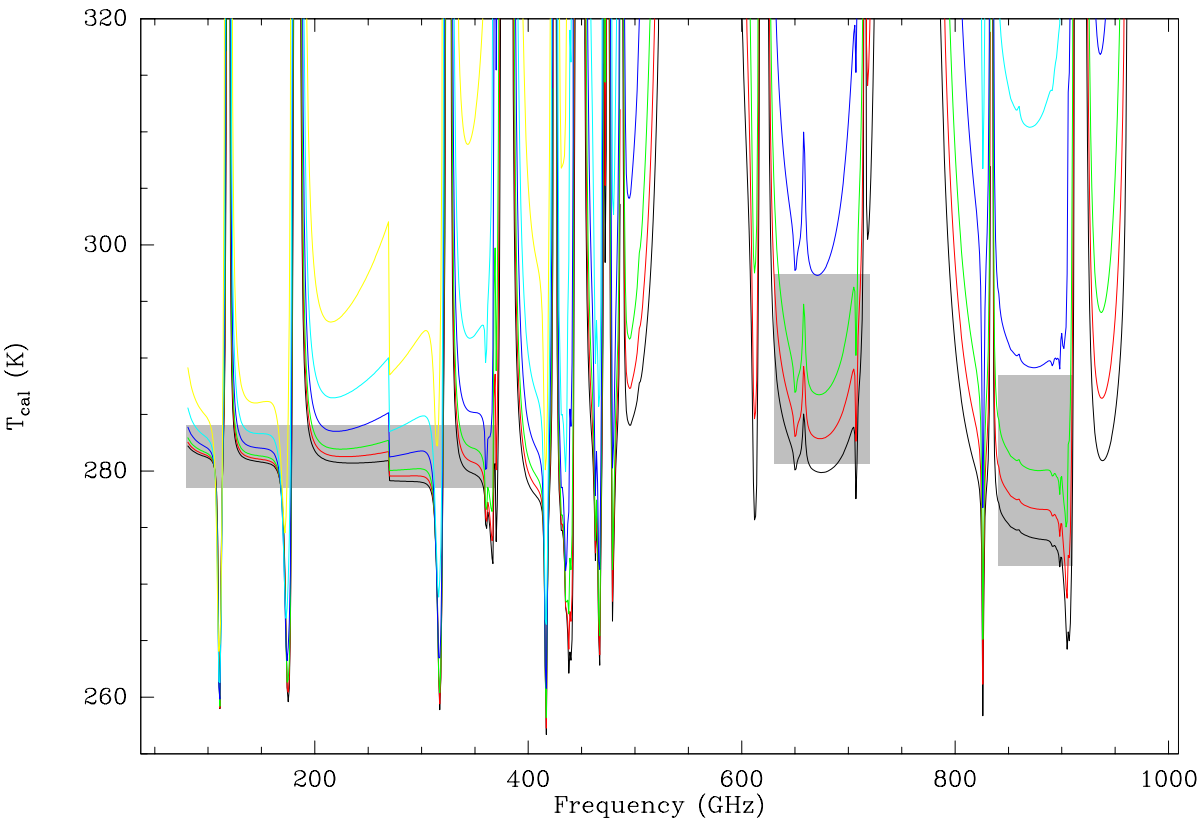

Figure 6: Dependency of the $T_{\rm cal}$ factor as function of elevation and frequency for a load temperature of 283 K. Curves are given for 6 airmasses: 1 (black), 1.2 (red), 1.44 (green), 2 (blue), 3 (cyan) and 5(yellow), corresponding to elevations of $90°, 56°, 44°, 30°, 19°$ and $11°$ respectively. The grey areas indicate the ± 1 % error level for Band 3, 6 and 7, and the ± 3% error level for Band 9 and 10.

[Bock et al. memo 225]
Bock, D., Welch, W.J., Fleming, M. & Thornton D., 1998
Radiometric Calibration at the Cassegrain Secondary Mirror *ALMA memo 225*

[Tucker & Feldman 1985]
Tucker, J.R, Feldman, M.J. 1985
Quantum Detection at Millimeter Wavelengths
Review of Modern Physics, 57, 1055-1113

[Ulich & Haas, 1976]
Ulich, R. & Haas, R.W., 1976
Amplitude Calibration of Millimeter Wavelengths Spectral Lines
ApJ Supp. 30, 247

[Guilloteau & Moreno, memo 371]
Moreno, R., & Guilloteau, S. 2001,
Receiver Calibration Schemes for ALMA *ALMA memo 371*

[Moreno & Guilloteau, memo 372]
Moreno, R., & Guilloteau, S. 2002,

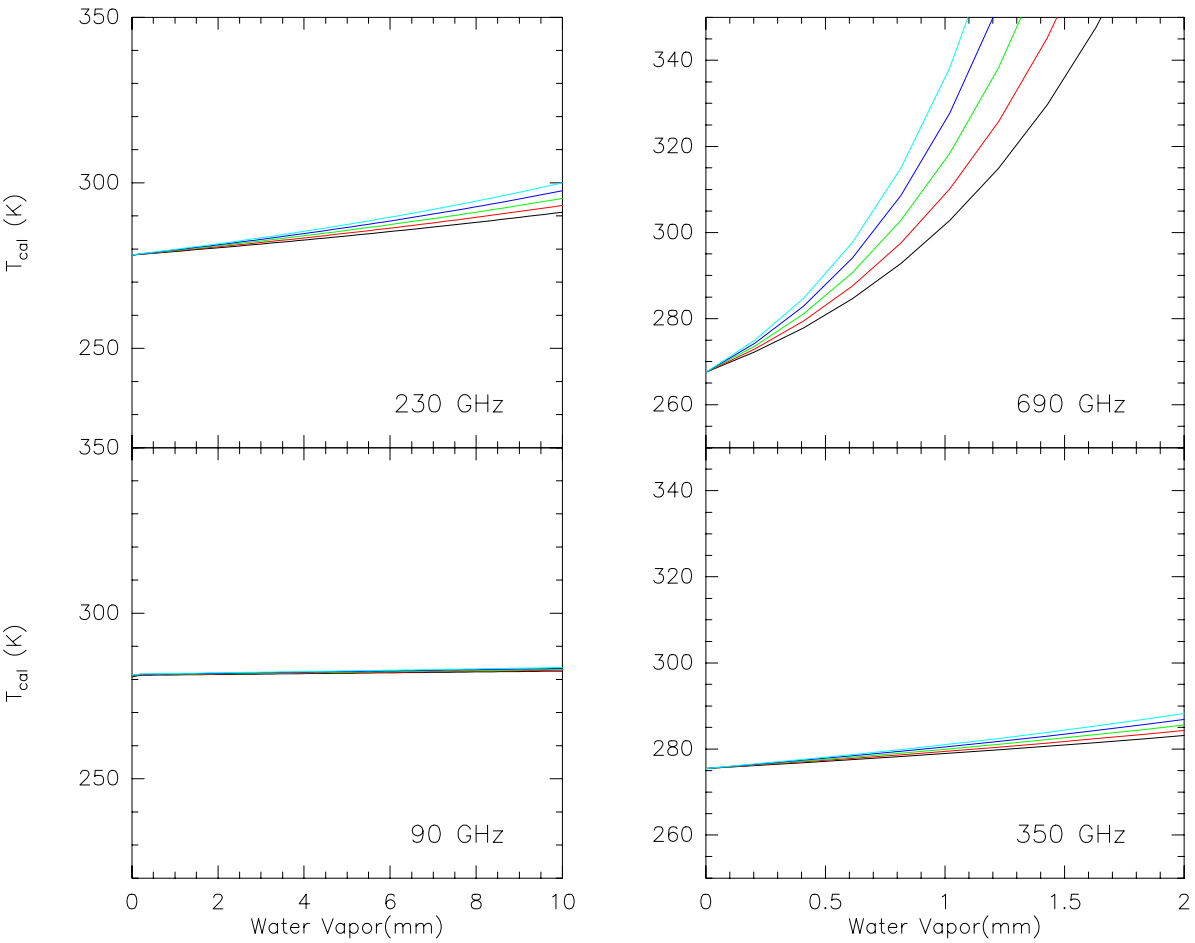

Figure 7: Dependency of the $T_{\rm cal}$ factor as function of water vapor content. The various curves are for different elevations.

ALMA Calibration: Requirements on the integration times, and suggested observing strategies. *ALMA memo 372*

[Kerr memo 401]
Kerr, A.R., 2002
Saturation by Noise and CW Signals in SIS Mixers. *ALMA memo 401*

[Guilloteau, memo 422]
Guilloteau S.,
The dual-load calibration system revisited. *ALMA memo 422*

[Guilloteau, memo 423]
Guilloteau S.,
The vane calibration system revisited. *ALMA memo 423*

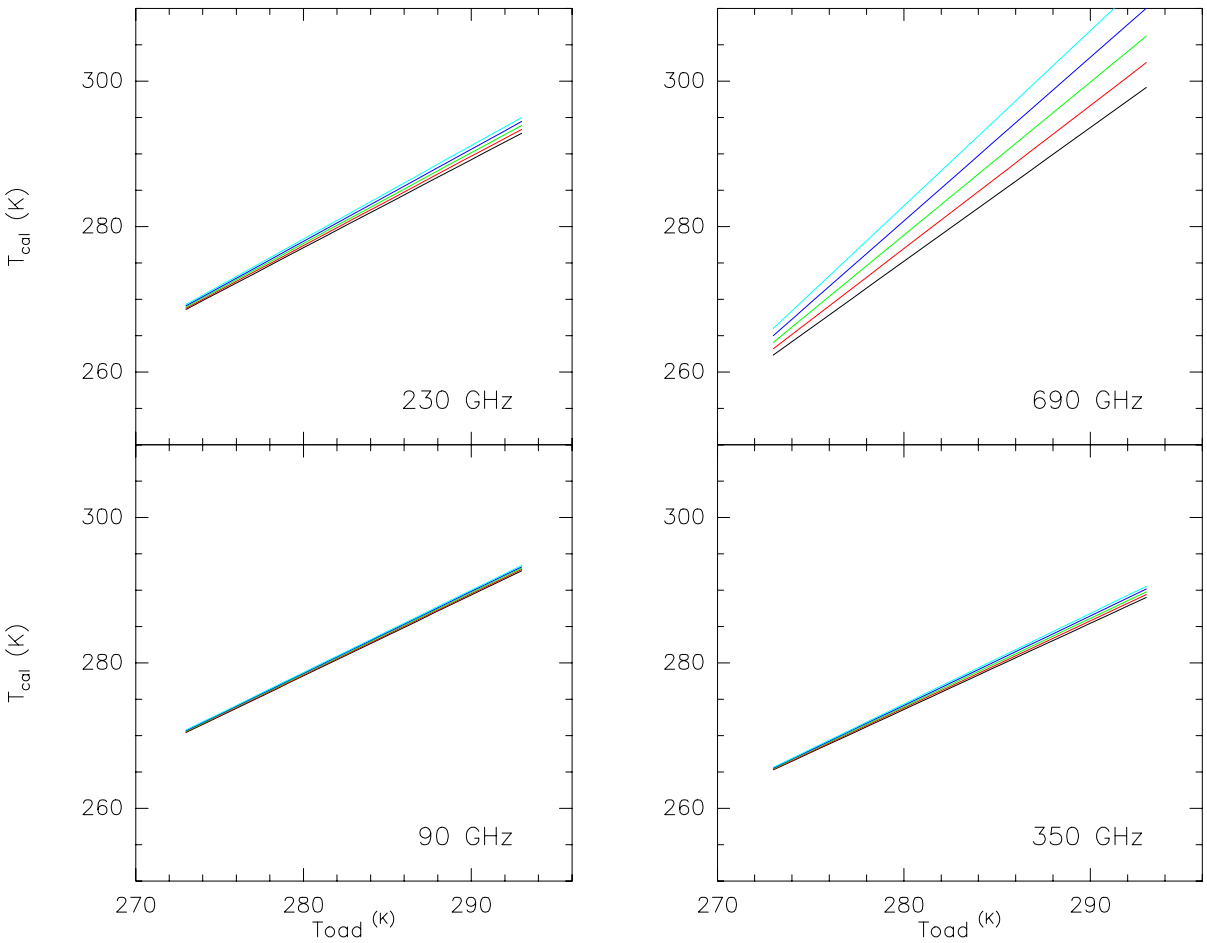

Figure 8: Dependency of the $T_{\rm cal}$ factor as function of load temperature. The various curves are for different elevations.